ETH zürich

ETH Library

Precombustion CO2 Capture by Pressure Swing Adsorption (PSA): Comparison of Laboratory PSA Experiments and Simulations

Journal Article

Author(s):
Schell, Johanna; Casas, Nathalie; Marx, Dorian; Mazzotti, Marco

Publication date:
2013-06-19

Permanent link:
https://doi.org/10.3929/ethz-b-000069065

Rights / license:
In Copyright - Non-Commercial Use Permitted

Originally published in:
Industrial & Engineering Chemistry Research 52(24), https://doi.org/10.1021/ie3026532

This page was generated automatically upon download from the ETH Zurich Research Collection.
For more information, please consult the Terms of use.

I&EC research
Industrial & Engineering Chemistry Research

Article

pubs.acs.org/IECR
Terms of Use

Precombustion CO_2 Capture by Pressure Swing Adsorption (PSA): Comparison of Laboratory PSA Experiments and Simulations

Johanna Schell, Nathalie Casas, Dorian Marx, and Marco Mazzotti*

Institute of Process Engineering, ETH Zurich, Sonneggstrasse 3, 8092 Zurich, Switzerland

Supporting Information

ABSTRACT: Pressure swing adsorption (PSA) experiments are carried out in a 2-column laboratory setup using activated carbon. As feed an equimolar CO_2/H_2 mixture is used. Adsorption pressures of 10, 20, and 30 bar are applied, whereas the desorption pressure and the feed temperature are fixed at 1 bar and 25 °C, respectively. During the experiments the temperatures at five different locations inside the columns are measured and the composition of the product streams is analyzed by a mass spectrometer. A one-dimensional, nonisothermal, nonequilibrium model is used to reproduce the experiments. The model was validated previously using breakthrough experiments, and the modifications required to describe full PSA cycles are highlighted. It is shown that the temperatures measured inside the columns provide an excellent possibility for comparison of experiments and simulations, whereas the measured concentration profiles are affected by the piping between column outlet and MS, which has to be considered carefully.

Downloaded via ETH ZURICH on August 26, 2022 at 06:50:22 (UTC).
See https://pubs.acs.org/sharingguidelines for options on how to legitimately share published articles.

INTRODUCTION

CO_2 capture and storage (CCS) is one option to reduce CO_2 emissions from large point sources, especially power plants.[1] This is in particular of importance considering the contribution of atmospheric CO_2 to global warming and climate change and the worldwide increasing energy demand, which will be based partly on fossil fuels in the medium term. Furthermore, coal is one of the fossil energy carriers that is still easily available and therefore the concept of precombustion CO_2 capture within an integrated gasification combined cycle (IGCC) power plant is of interest. In this concept, a solid fuel, in general coal, is gasified with O_2 and converted in a water gas shift (WGS) reactor to the main components H_2 and CO_2. The high pressure of around 35 bar and the high CO_2 mole fraction of approximately 40% on a dry basis make the removal of CO_2 at this point easier from a thermodynamic point of view as compared to the so-called postcombustion capture scheme where CO_2 is removed from the flue gas (typically 3−13 mol % CO_2 and 1 bar total pressure). However, in order to enable the application of CCS, the energy penalty of the capture step is crucial and has to be decreased.

Among the different technologies under development for precombustion CO_2 capture, pressure swing adsorption (PSA) looks promising due to the inherently low energy consumption if the feed stream is already at high pressure as in this case. One of the characteristics of PSA are the many design options: beside selecting a suitable adsorbent material for the desired separation and additional to fixing the pressure and temperature of the process, the different process steps can be combined in a variety of ways, using different streams, in order to define the so-called cycle. Therefore, a model-based design is especially beneficial to avoid huge experimental efforts. Such models consist in general of mass, energy, and momentum balances combined with thermodynamic equations to describe the properties of the fluid and adsorbed phase as well as the equilibrium between these two. In order to use the model, several model parameters have to be determined and adapted to the specific conditions of interest (adsorbent−adsorbate combinations, pressures, temperatures, flow rates, etc.). Equilibrium properties such as adsorption isotherms are usually measured independently, whereas the dynamic model parameters (e.g., mass or heat transfer parameters) are commonly fitted to dynamic column experiments. In most cases, breakthrough experiments are used for this fitting, as we also have shown in a previous study.[3] Breakthrough experiments represent very closely the conditions during the adsorption step of a PSA cycle. However, during a complete PSA cycle different steps with different characteristics such as blowdown, purge, or pressure equalization are encountered and the model with its parameters should describe them equally well. Therefore the comparison between experimental results of full PSA cycles with simulation results is an important step in the validation of the model and a prerequisite for its use for process development.

In this work, PSA experiments in a fully automated laboratory two-column setup at 25 °C and at three different adsorption pressure levels, namely 10, 20, and 30 bar, are performed. The desorption pressure is always 1 bar. A commercial activated carbon is chosen as adsorbent material, which has already been characterized in previous studies.[3,4] As feed, an equimolar gas mixture of CO_2 and H_2 is used, which is similar to the typical feed in a precombustion CO_2 capture context when impurities are neglected. The PSA cycle consists of the following steps: pressurization, adsorption, blowdown, purge, and pressure equalization. During the experiments the temperature profiles inside the columns are inline monitored by several thermocouples and the composition of the high and low

Received: September 28, 2012
Revised: May 7, 2013
Accepted: May 24, 2013
Published: June 7, 2013

 © 2013 American Chemical Society dx.doi.org/10.1021/ie3026532 | Ind. Eng. Chem. Res. 2013, 52, 8311−8322

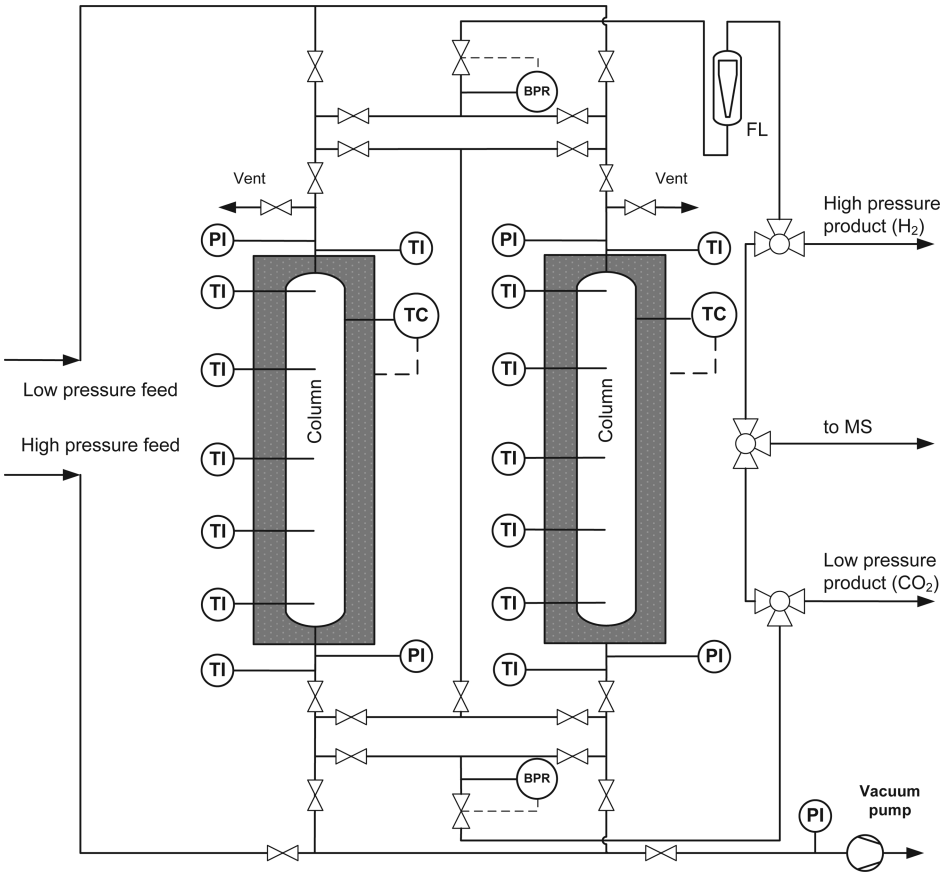

Figure 1. Laboratory two-column PSA setup.

pressure products is analyzed online by a mass spectrometer (MS). In this context it is worth mentioning, that it is not the aim of this study to present a PSA cycle which is optimal for CO_2 capture but to validate the process model which is then used to compare different process schemes, cycles, conditions, and configurations. Hence, CO_2 purity and recovery are not optimized when choosing the experimental conditions.

However, as the purity of the two products and the capture rate of CO_2 are the quantities used to evaluate the process performance, it is necessary to validate the model with respect to these metrics. To this end, additionally to the experiments described above, a separate series of experiments have been performed wherein only the length of the adsorption step is varied. During these experiments, the flow rate of the H_2-rich product is measured during the adsorption step of each cycle. In combination with the composition measured by the MS and knowing the feed flow rate and composition, this allows for the determination of the total purity and recovery of the H_2 product, and through the mass balance also of the corresponding CO_2 purity and capture rate. Rather than measuring the flow rate and composition of the CO_2 product, it was decided to use the H_2 stream, as its flow rate and composition are relatively constant throughout the adsorption step, thus enabling a more reliable measurement.

To simulate the process, a one-dimensional, nonisothermal, nonequilibrium model is used, whose transport parameters have been estimated previously by fitting single-column breakthrough experiments.[3] The same model has been applied to simulate variations of the PSA process such as different cycle configurations and different conditions within the context of precombustion CO_2 capture.[5] In this work, simulation results are compared to PSA experiments and the agreement or discrepancy is discussed. Thus, the validation and assessment of the model in the context of the complete PSA process is obtained.

■ EXPERIMENTAL SECTION

Materials. The adsorbent material used in this work is a commercial activated carbon (AP3-60 from Chemviron Carbon, Germany), which has already been characterized in previous studies.[3,4] In agreement with the procedure reported in Schell et al.[4] the cylindrical pellets (diameter of 3 mm) are fully regenerated under vacuum at 150 °C for 8 h before the first experiment. Between experiments a moderated regeneration is applied using only vacuum for 45 min, which is shown in a previous study to be sufficient.[3] The density of the material is determined to be 1965 kg/m^3 by helium pycnometry (AccuPyc 1330, Micrometritics, Belgium), whereas the particle density is 850 kg/m^3 as specified by the manufacturer.

As feed to the PSA unit, gas mixtures with relative errors of ±0.5 to 3.0% are used, which are prepared by Pangas (Dagmersellen, Switzerland) from the pure gases at purities of 99.9% for CO_2 and 99.999% for H_2.

Experimental Setup. The one column adsorption setup described in a previous study[3] is expanded with a second similar column in order to allow for full PSA experiments including one pressure equalization step. A flowsheet of the main parts (without feeding and analyzing section) is shown in Figure 1. In the following, the key features of this setup are repeated and the modifications compared to the work of Casas et al.[3] are

highlighted. Furthermore, the setup dimensions together with the physical properties of the bed and the adsorbent material are summarized in Table 1.

Table 1. Setup Dimensions and Physical Properties of the Bed and Adsorbent Material[a]

column length	L	[m]	1.2
internal radius	R_i	[m]	0.0125
external radius	R_0	[m]	0.02
heat capacity wall[b]	C_w	[J/(K m^3)]	4×10^6
material density	ρ_M	[kg/m^3]	1965
particle density	ρ_p	[kg/m^3]	850
bed density	ρ_b	[kg/m^3]	480
particle diameter	d_p	[m]	0.003
heat capacity adsorbent	C_s	[J/(K kg)]	1×10^3

[a]Each bed is packed with about 280 g of adsorbent material. [b]Value lumping column wall and heating layers.

In order to provide the feed flow to the columns, two mass flow controllers (MFC) (Bronkhorst High-Tech BV, The Netherlands), one for the high and one for the low pressure feed, are applied. For each column, five thermocouples (Moser TMT AG, Switzerland) at different axial locations in the adsorbent bed as well as one thermocouple at each inlet and outlet monitor the temperature during the process, whereas the electrical heating of the columns is controlled by an additional thermocouple installed at the wall. The positions of the thermocouples in the columns are from bottom up at 10, 35, 60, 85, and 110 cm. Both columns are insulated (Insultech AG, Switzerland). The pressure at the inlet and outlet of the two columns is recorded by pressure transducers (Keller, Germany). In contrast to the setup used for breakthrough experiments with constant pressure during the entire experiment,[3] two automated back pressure regulators (BPR) (Bronkhorst High-Tech BV, The Netherlands) are employed to control the pressure levels in the columns during the different steps. The whole setup, including the time scheduling of the individual steps during a PSA cycle, is controlled by LabVIEW (National Instruments Corporation, Texas, USA) in order to enable a smooth, automated and reproducible operation during the PSA experiments. Therefore, automatic valves are installed at all positions where they have to be opened and closed periodically during a PSA cycle. The compositions of the high and low pressure products are online measured sequentially using a mass spectrometer (MS) (Pfeiffer Vacuum Schweiz AG, Switzerland); first the composition of the high pressure H_2 product is measured for several cycles until the MS connection is switched in order to measure the low pressure CO_2 product. During the experiments performed to determine the process performance, a Messglas V-100 rotameter (Vögtlin instruments, Switzerland) is used to measure the flow rate of the H_2 product during the adsorption step. The rotameter is installed between the BPR and the valves determining which product is analyzed by the MS, as is illustrated in Figure 1 (labeled "FL").

Experimental Procedure. PSA experiments at 25 °C and at three different adsorption pressures p_{high}, namely 10, 20, and 30 bar, are carried out. In all cases, the desorption pressure p_{low} is maintained at 1 bar. For both columns, the schedule applied in the experiments in this work is shown schematically in Figure 2, whereas the cycle sequence for one column is illustrated in Figure 3. The following steps are involved in the process:

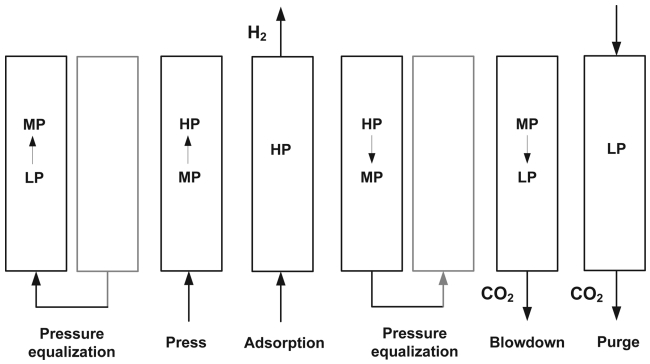

Figure 3. Cyclic sequence of the PSA process investigated in this work. The cycle is shown for one column only (black column). LP and HP are the low pressure (p_{low}) and high pressure (p_{high}), respectively, whereas MP is the intermediate pressure (p_{peq}) corresponding to the pressure equalization step.

- *Adsorption*: at p_{high}, characterized by a constant volumetric feed flow rate, production of high pressure H_2 product, bottom up flow;
- *Pressure Equalization* (Peq): the high pressure column after the adsorption step is connected to the low pressure column after the purge step until both columns reach the same intermediate pressure p_{peq}; it is conducted in the same direction as the pressurization and blowdown steps, respectively;
- *Blowdown*: reduction of the pressure from p_{peq} down to p_{low}, run countercurrently to the adsorption step, production of low pressure CO_2 product;
- *Purge*: at p_{low}, a constant feed flow is adjusted countercurrently to the adsorption step, low pressure CO_2 product is produced;
- *Pressurization*: increase of the pressure from p_{peq} up to p_{high}, run cocurrently to the adsorption step.

The length of the two idle steps I1 and I2 shown in Figure 2 depends on the duration of the other steps and their relation, which are summarized in Table 2. As mentioned before, these times are not chosen in order to optimize CO_2 purity and capture rate, as it is not the aim of this study to present a PSA cycle which is optimal for CO_2 capture but to build an experimental database for the validation of the process model.

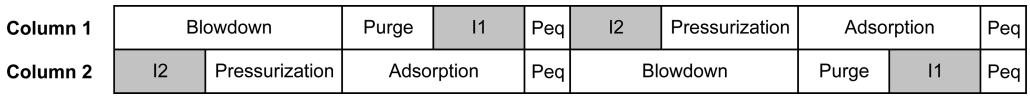

Figure 2. PSA cycle implemented in this work. The rows show the two columns, and time runs from left to right (see Table 2 for the duration of the individual steps).

Table 2. Times of the Individual Steps of the PSA Experiments and Experimental process performance[a]

p_{high} [bar]	t_{press} [s]	t_{ads} [s]	t_{peq} [s]	t_{blow} [s]	t_{purge} [s]	H_2 purity [%]	H_2 recovery [%]	CO_2 purity [%]	CO_2 recovery [%]
10	30	40	3	30	15				
20	24	40	3	50	15				
30	28	35	3	55	15				
20	24	20	3	50	15	95.2 ± 1.5	62.0 ± 5.8	71.9 ± 4.3	96.9 ± 5.8
20	24	40	3	50	15	93.4 ± 1.5	74.4 ± 5.7	78.7 ± 4.7	94.8 ± 5.7
20	24	60	3	50	15	88.5 ± 1.5	93.0 ± 5.5	92.6 ± 5.7	88.0 ± 5.4
20	24	100	3	50	15	71.8 ± 1.5	93.8 ± 3.5	91.1 ± 5.1	63.1 ± 3.5
20	24	100	3	50	15	72.5 ± 1.5	95.4 ± 3.7	93.4 ± 5.4	63.9 ± 3.7

[a]The experiment with t_{ads} = 100 s was performed twice, while purity and recovery were not measured for three of the experiments.

As feed to the adsorption and pressurization step, an equimolar mixture of CO_2 and H_2 is used. Because for the application considered in this study it is not the aim to produce a highly pure H_2 stream, the same feed is taken in the purge step. This is in contrast to traditional H_2 PSA where typically a part of the high purity H_2 product is used in the purge step. The volumetric feed flow rate in the adsorption and purge steps is 20 and 50 cm^3/s, respectively, for all experiments. However, it is worth keeping in mind that the feed to the adsorption step in terms of molar flow changes depending on the pressure. A special discussion is required for the volumetric flow rate in the pressurization step. The set point given to the MFC during pressurization is the same as during adsorption. However, due to the measurement principle of the MFC, which is based on thermal conductivity and heat capacity of the gas, the actual flow rate depends on pressure, temperature and gas composition. As the pressure is changing during the whole pressurization step, the flow rate is only approximately 20 cm^3/s.

Directly before each experiment the MS is calibrated using the feed gas mixture (50% CO_2, 50% H_2) at 1 bar. The experiments are run long enough to ensure periodic steady state conditions for several cycles, i.e. for every experiment 20–30 cycles are performed. Experiments at one specific condition are repeated at least once in order to check reproducibility.

Determination of Process Performance. For the validation of the model regarding the process performance, i.e. CO_2 purity and capture rate, a series of experiments is performed at an adsorption pressure of 20 bar. The timing of the individual process steps is identical with the exception of the duration of the adsorption step t_{ads}, for which values of 20, 40, 60, and 100 s are used, the last experiment being performed twice to verify the reproducibility. Due to the strongly changing composition and flow rate during the CO_2-producing steps, particularly the blowdown, the process performance is assessed based on the H_2-rich product. To find the amount of each component that is fed to each column throughout a cycle, the feed flow rate recorded by both MFCs is integrated over the duration of the pressurization, adsorption, and purge steps. The amount of H_2 product is found by measuring the flow rate of the H_2 product during the adsorption step. As the position of the float is strongly dependent on the density of the flowing gas, and thereby the composition, a calibration using mixtures of known composition was performed. Once the cyclic steady state has been reached, a video camera is used to record the position of the rotameter float throughout the duration of at least three consecutive process cycles. During the adsorption steps, the reading is noted at least every five seconds, more frequently when needed. Using the composition of the product gas as measured by the MS to calculate the density, and the previously performed calibration of the rotameter, the volumetric and molar flow rates of the stream are calculated. The molar flow rates of each component are then integrated to find the total amount of each component in the H_2 product. The CO_2 product stream is then found by subtraction from the amount fed. The purity and capture rate of the CO_2 can thus be found. As the calculation is performed for each column individually over three process cycles, a total of six values is obtained, from which the mean is calculated. Further detail is given in the Supporting Information.

Modeling. The PSA process is described by a one-dimensional, nonisothermal, nonequilibrium model. It is validated and discussed in detail in previous publications in the context of the description of experimental breakthrough experiments[3] and of the evaluation of PSA cycles as a precombustion CO_2 capture process.[5] The model used in this work combines characteristics from both studies, i.e. all aspects related to the experimental setup, e.g. the description of the column wall heat balance, are taken from the work of Casas et al.[3] whereas the description of the pressure changing steps is done based on the work of Casas et al.[5] For the sake of completeness, the assumptions made in the derivation of the model equations are listed again here:

- Radial gradients of temperature, concentration and velocity are neglected following an analysis based on the approach presented by Farooq and Ruthven;[2] this shows that the value of the dimensionless radial thermal conductivity is in our experiments always equal to or larger than the critical threshold proposed in that work;
- Between the fluid and the adsorbent material, thermal equilibrium is established;
- The fluid phase behavior is described by the ideal gas law; this is reasonable considering that the compressibility factor calculated using the Peng–Robinson equation of state (EOS) is still >0.9 at 30 bar and 75% CO_2 as shown in a previous study;[3]
- Axial dispersion and conductivity are neglected; their influence on the overall PSA process is negligible as observed in a previous study[5] where this issue was investigated in great detail;
- The column wall and metal layers of the heating system are combined using lumped parameters;
- The ambient temperature is kept constant at T_{amb} = 25 °C;
- The linear driving force model (LDF) is used to describe the mass transfer upon adsorption;
- Mass transfer coefficients, heat of adsorption, and heat capacities (C_s, C_w, and $C_{g,i}$) are constant and independent of temperature;

- Constant average values are used for the thermal conductivity and the viscosity of the fluid;
- The momentum balance is reduced to a pressure drop relation (Ergun equation);
- Kinetic and potential energies are neglected in the energy balance.

The set of partial differential equations resulting from the mass, energy, and momentum balances and the additional algebraic equations are summarized in the Supporting Information. The adsorption equilibrium is described by an empirical competitive Sips isotherm, which has shown to predict experimental binary equilibrium data reasonably well with the parameters summarized in the Supporting Information. Using the isotherm data in combination with the Clausius−Clapeyron equation, the value of the isosteric heat depends on the amount adsorbed as well as on the temperature.[4] However, in this study, a constant value is selected (as reported in the Supporting Information), whose choice will be discussed in the next section. In Table 3, the values of all remaining model parameters are given as determined in the breakthrough study.[3] This is true except for the values of η_1 and η_2, which will be discussed in the next section. Details of the numerical implementation, the realization of the pressure equalization step, and the boundary conditions can be found elsewhere.[3,5]

Table 3. Model Parameters: Values of k_i and h_w Used As Determined in the Work of Casas et al. and,[3] for η_1 and η_2, the Original Parameters from Leva's Correlation[10,11]

		CO_2	H_2
k_i	[1/s]	0.15	1.0
$C_{g,i}$	[J/(K mol)]	42.5[a]	29.0[a]
μ	[Pa s]	1.46×10^{-5} [b]	
K_L	[W/(m K)]	0.04[b]	
h_w	[W/(m^2 K)]	5	
η_1	[−]	0.813	
η_2	[−]	0.9	

[a]Average value taken for the conditions (pressure and temperature) encountered in the experiments.[13] [b]Average value taken for an equimolar mixture of CO_2 and H_2 at 30 °C and 15 bar.[14]

Apart from the discussion above, two points are changed and adjusted in order to allow for a more realistic description of the experimental results in this study. The first point concerns the boundary conditions at the open end, i.e. at the outlet or inlet, during the blowdown and pressurization steps, respectively. In practice during pressurization the flow rate is controlled by the MFC (see above), whereas during blowdown the outlet pressure, i.e. after the valves and piping following the adsorption columns, is kept constant. None of these experimental techniques of operating pressurization and blowdown can be directly translated into boundary conditions for the adsorption beds; therefore, we have considered using pressure−time profiles, extracted from experimental measurements, as boundary conditions. Indeed we have verified that these are numerically effective and accurate enough. This approach is in fact adopted in several studies[7−9] and is therefore used in this work as well. The functions describing the pressure with time are as follows, where the factor ξ is a fitting parameter and t is the time since the start of the corresponding step:

Blowdown

$$p(x = 0;\, t) = p_{\mathrm{low}} + (p_{\mathrm{peq}} - p_{\mathrm{low}})\exp(-\xi t) \tag{1}$$

Pressurization

$$p(x = 0;\, t) = p_{\mathrm{peq}} + \frac{p_{\mathrm{high}} - p_{\mathrm{peq}}}{t_{\mathrm{press}}} t \tag{2}$$

The second modification is related to the idle steps. In order to be more consistent with the experimental procedure, these steps are included in the model assuming no flow into the column or out of it. However, processes related to transfer resistances (mass or heat transfer) are allowed during these steps.

As already discussed in the work of Casas et al.,[3] the piping between the column outlet and the measurement position at the MS has to be considered in order to allow for a meaningful comparison between experiments and simulations in terms of composition. To this aim, a simple time correction of the experimentally measured data is not possible because of several effects such as changing flow rates. Therefore, also in this study, it is accounted for in the model by describing the piping with an isothermal plugflow model. However, due to the changing pressure, flow rates, and idle steps, in the PSA case the situation is more complex than in the breakthrough experiments. This issue is analyzed in more detail in the next section.

■ RESULTS AND DISCUSSION

Experimental Results. The experimental results at steady state in terms of pressure before and after the column, temperatures at the five positions inside the column, and composition measured at the MS during the production of the high and low pressure product, i.e. H_2 and CO_2, respectively, exhibit an excellent reproducibility. In order to confirm this, a comparison between different cycles, different columns, and different experiments at 20 bar is provided in Figures 4 and 5. The same figures are also used for a general discussion of the typical experimental results.

In Figure 4a, the pressure profiles measured before and after the column during one cycle are compared, which are indicated by the symbols and the line, respectively. It can be seen that there is hardly any difference between these data suggesting that the pressure drop over the column is rather low even in the pressure changing steps, such as pressurization or blowdown. The pressure profiles of different cycles and experiments as well as for all three different values of p_{high} are used to fit the parameter ξ of eq 1, and it is found that the experimental results can be well described with a value of $\xi = 0.28$.

The temperature profiles at the five thermocouple positions during one cycle are shown in Figure 4b. In this case, symbols and lines represent two different independent experiments and the excellent agreement confirms the reproducibility of the measurements. Moreover, as the shown temperature profiles are taken from different cycles numbers with respect to the start of the experiment, the agreement confirms the assumption of cyclic steady state. The temperatures inside the column are increasing during the pressurization and adsorption steps. This process starts at the column inlet and is therefore observed first at the thermocouples at 10 and 35 cm (squares and triangles), followed by the thermocouples at 60 and 85 cm (circles and stars). It corresponds directly to the CO_2 adsorption front traveling through the column as it was already shown in the breakthrough experiments.[3] At 110 cm (diamonds) only a

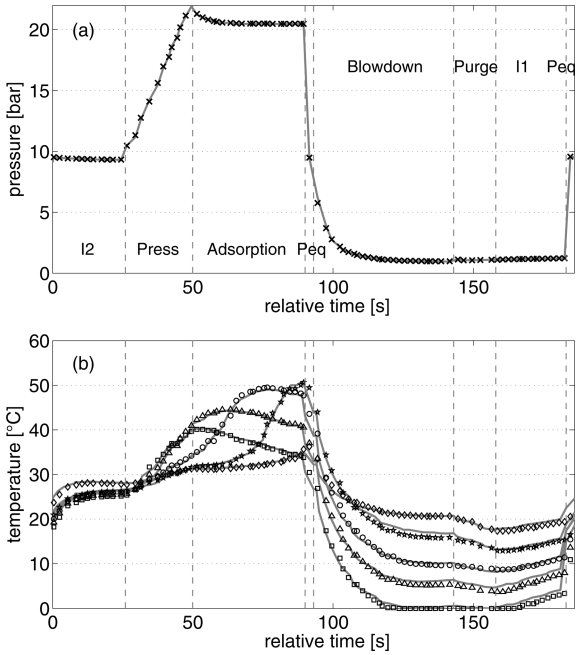

Figure 4. Typical experimental pressure and temperature profiles at 20 bar. (a) Pressure profiles before and after the column indicated by the lines and the symbols, respectively. (b) Temperature profiles measured during one cycle. Symbols and lines represent two different independent experiments and are taken from different cycle numbers with respect to the start of the experiment. The temperatures are measured at the following positions from the column bottom: (squares) 10; (triangles) 35; (circles) 60; (stars) 85; (diamonds) 110 cm.

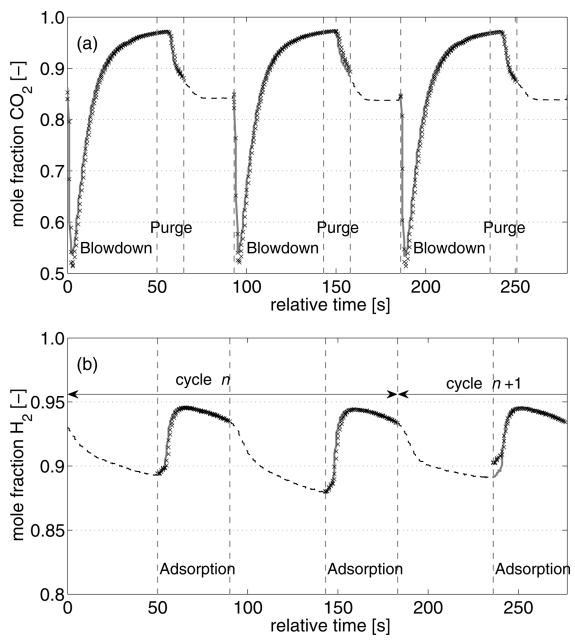

Figure 5. Typical experimental composition profiles during one and a half cycles at 20 bar: (a) CO_2 product; (b) H_2 product. In both cases, two experiments are compared represented by the symbols and the solid gray line (dashed line: measurement during the breaks when no product is produced).

slight increase of the temperature at the end of the adsorption step is observed, which indicates that the CO_2 front is just about to reach this position. After equilibrium is established at one position in the column, the temperatures start again to decrease due to the heat exchange with the wall and the surroundings. This becomes evident for positions 10 and 35 cm (squares and triangles). At a certain time during the adsorption step, the temperatures measured at these positions reach a maximum, which is followed by an almost linear temperature decrease. During blowdown and purge, the opposite phenomenon is observed: the temperatures in the column are decreasing caused by the desorption, which starts at the open end of the column during blowdown, i.e. close to the thermocouple at position 10 cm. It can be seen that after about half of the blowdown time the temperatures approach a constant value, which can be explained by the fact that the pressure in the column is already at 1 bar (see Figure 4a). Therefore, the desorption rate is lower as compared to the initial phase of the blowdown and the temperature decrease associated with it only compensates for the heat exchange with the column wall. During purge, the desorption is again increased slightly, which is reflected by the decrease in temperature. As it can be seen from this discussion, the temperatures at the different positions inside the column provide very useful and important information about the adsorption process. This will be exploited also in the following when experiments and simulations are compared.

In Figure 5, the composition profiles of the CO_2 and H_2 product as measured with the MS are shown. Again two different independent experiments are compared, indicated by the symbols and the lines, and the agreement is very good. Note that only one product stream can be measured at the same time (compare Figure 1). First the H_2 product is measured for several cycles before the MS connection is switched to measure the CO_2 product. Furthermore, during one cycle the selected product, i.e. CO_2 or H_2, is produced from both columns in an alternating way, which means that Figure 5 represents one and a half cycles. In this way, by looking at two consecutive blowdown, purge, or adsorption steps the two columns can be compared. Also this comparison is very satisfying, which shows that the two columns indeed behave the same.

The low pressure CO_2 product, as illustrated in Figure 5a, is produced in the blowdown and purge step. At the very beginning of the blowdown step, the composition measured still corresponds approximately to that measured at the end of the preceding purge step, but it is decreasing rather steeply down to a value close to the feed composition of the adsorption step. When looking at the process cycle (Figure 2), this can be explained by the fact that the blowdown follows the adsorption and pressure equalization steps. During the blowdown the CO_2 mole fraction is then increasing as more and more CO_2 desorbs. Since the feed mixture (50% CO_2/50% H_2) is used in the purge step, the CO_2 mole fraction is finally again decreasing because of the diluting effect. After the purge step, for a certain time no CO_2 is produced until the blowdown step of the other column starts (compare also with Figure 2). Nevertheless, during this "pause" the MS is still measuring and the observed values, which are indicated by the light dashed line in Figure 5a, correspond to the composition at the end of the piping system. They can be regarded as a kind of measurement artifact, which alter slightly the starting point in the next blowdown step but have no big impact in the case of the CO_2 product. The situation is different for H_2, as discussed in the next paragraph.

In Figure 5b the high pressure H_2 product is shown. It is produced during the adsorption step only. For the following discussion, it is worth highlighting that the scale of the vertical axis for the H_2 product is smaller than for the CO_2 product; therefore, all discrepancies are more pronounced for H_2. As in the case of the CO_2 product, after one column has finished the adsorption step no H_2 is produced for a certain time until the other column starts with the adsorption step (see Figure 2). The signal measured during the pause by the MS is again represented by the light dashed line. In this case, the influence of that effect is more important, because it is not the same in all steps as it can be seen in Figure 5b. Furthermore, it influences the signal measured at the beginning of the adsorption step as explained in the following. At the end of the adsorption step the pipe from the column outlet to the MS is filled with a gas of about 94% H_2. We believe that during the pause some of this H_2 is selectively leaking out of the pipe and in this way the H_2 mole fraction is decreased. When the new adsorption step starts, first this gas with a lower H_2 content has to be pushed out of the piping before the gas from the outlet of the column with higher H_2 content reaches the MS. In the case of adsorption this takes longer compared to the blowdown step, because the velocity at the column exit is much smaller. Consequently, the first part of the measured H_2 product (increase of the concentration) is the result of the measurement procedure and of the setup after the adsorption column, rather than representing the composition at the outlet of the adsorption column itself.

Comparison to Simulation Results. The comparison of experimental and simulation results is based on the cyclic steady state conditions. As already mentioned above, the composition measured at the MS does not correspond directly to the gas coming out of the columns, but is influenced by the piping and the time without production (pause). Moreover, the preceding steps can play a role, for instance the pressure equalization step uses partly the same piping as the following blowdown step. In the work of Casas et al.[3] the importance of describing the piping after the column in order to be able to compare measured and simulated concentration profiles is discussed in detail. In the case of PSA experiments this issue is even more important and complex, because of the additional piping structure in the two column setup and also of the changing pressure and velocity, for instance in the blowdown step. On the other hand, the temperature profiles are measured without delay inside the columns at specified locations and, as explained before, they are linked directly to the adsorption and desorption processes at these positions. Therefore, comparing the experimental and simulation results based on the temperature profiles is a convenient approach and will be exploited in the following. Additionally, the issues in comparing the composition profiles are discussed with an exemplary case.

Temperature Profiles. The temperature profiles at the specified five locations inside the column (10, 35, 60, 85, and 110 cm from the bottom column inlet) during one cycle for the experiments at 10, 20, and 30 bar are shown in Figure 6. Symbols represent the experiments whereas the lines are the simulation results. Taking into account the complexity of the whole process, the agreement is good. This is especially true for the experiment at 30 bar where the measured temperatures are very closely reproduced by the simulations. Slightly worse, but still acceptable, is the agreement at 20 bar. At 10 bar, in order to match experiments and simulations the feed flow rate applied in the simulation during the adsorption step has to be reduced to

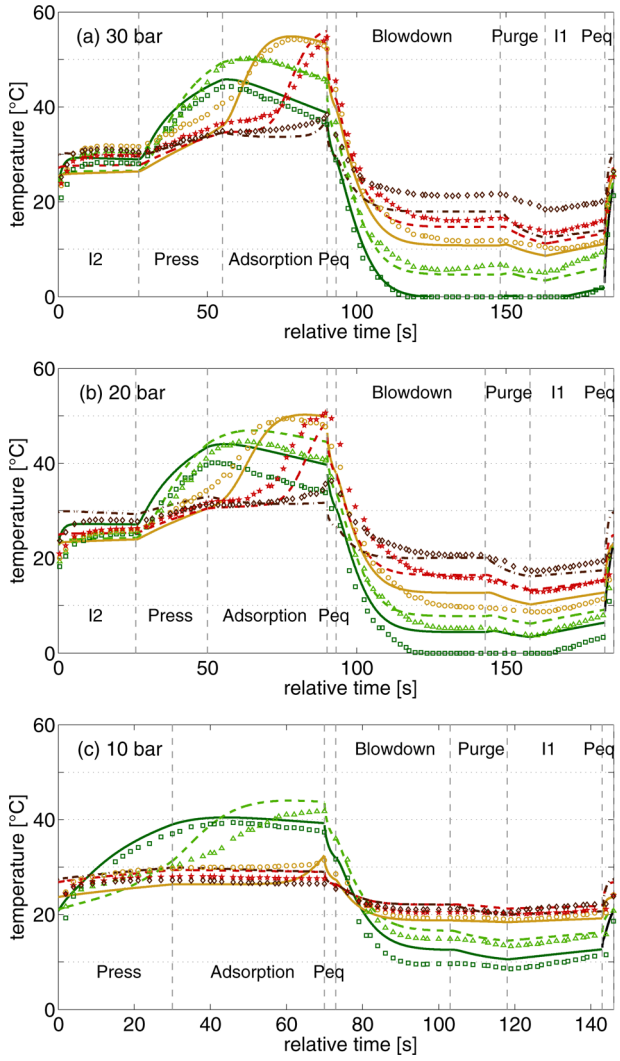

Figure 6. Comparison of temperature profiles: simulation and experiment at steady state at different pressures (symbols) experiments, (lines) simulation; from the column bottom: 10 (squares, dark green); 35 (triangles, light green); 60 (circles, yellow); 85 (stars, red); 110 cm (diamonds, brown).

17 from 20 cm^3/s as in the experiment. In the evaluation of the breakthrough experiments[3] it has already been observed that in some cases the feed flow rate adjusted in the experiments and the one used in the simulations disagree slightly. This might be caused by some experimental issues concerning the used MFCs, which are calibrated for specific conditions and might be less accurate at other conditions. Furthermore, in the case of the PSA experiments at 10 bar, the CO_2 adsorption front at the end of the adsorption step is just about to reach the thermocouple at position 60 cm. As a consequence, the experiment provides no details about the time when the CO_2 front would reach further positions in the column. This results in less information about the adsorption process at 10 bar as compared to 20 or 30 bar and makes the evaluation less reliable.

Two important changes in the simulations of the PSA experiments compared to those of the breakthrough study[3] have to be discussed. The first concerns the calculation of the heat transfer coefficient from inside the column to the wall, h_L. For the breakthrough experiments[3] the values of the two parameters η_1 and η_2 in the Nusselt correlation according to

Leva[10,11] (see Supporting Information) have been adapted in order to better match the experimental results. However, looking at the whole PSA cycle it turns out that in order to describe all steps equally well, the best choice is to use the original parameters from Leva's correlation,[10,11] which are reported in Table 3. For the calculation of h_L according to this correlation the density is calculated depending on the actual conditions in the column (dependent on time and space), whereas constant average values are applied for the viscosity and thermal conductivity. The latter simplification is consistent with the work of Casas et al.,[3] where additionally a constant superficial gas velocity is assumed for the calculation of the Reynold's number. However, in the PSA experiments the velocities are changing in a wider range and therefore a velocity dependent on time but not on space is used. More precisely, during the pressurization, the pressurization via pressure equalization, the purge, and the adsorption steps the inlet velocity at the actual time is used, whereas during the blowdown and the blowdown via pressure equalization steps the outlet velocity is used. This is an acceptable simplification, which improves the numerical stability significantly. The applied correlation for h_L does not assume any heat exchange when the velocity is zero, i.e. during the two idle steps. This is in contrast to the experimental observation, which shows clearly a temperature change (compare for instance I1 in Figure 6). Therefore, a value of $h_L = 20\ \mathrm{J/(K\ s\ m^2)}$ is assumed during the idle steps in order to match the experimental results.

The second change has to do with the value of the isosteric heat of adsorption of CO_2. In the work of Schell et al.[4] it has been shown that the isosteric heat of adsorption is dependent on temperature and loading. On the other hand, in process simulations often a constant average value is used. In the breakthrough study[3] a relatively high value of $\Delta H_{CO_2} = -26\,000$ J/mol is applied, which corresponds to rather low loading values. This seems reasonable as in the breakthrough experiments adsorption takes place in a completely regenerated column. In the case of PSA experiments, the situation is different. During blowdown and purge the column is only partially regenerated, which means that the adsorption sites exhibiting the highest heat of adsorption, corresponding to the strongest adsorption, will probably stay "occupied" and only sites with lower heat of adsorption are involved in the adsorption−desorption process. Consequently, in the PSA simulation a smaller average value for the isosteric heat of adsorption of CO_2 is selected, namely $\Delta H_{CO_2} = -21\,000$ J/mol, which leads to a very good agreement with the experimental results.

Pressure Equalization. One important aspect in a PSA simulation model is the description of the pressure equalization step where a column at high pressure, p_{high}, is connected to a second column at low pressure, p_{low}. The pressure level obtained at the end of this step, p_{peq}, is not only depending on the initial conditions of the columns, but also on the dynamics and the adsorption behavior during it. This is important to consider because the subsequent steps are influenced by this pressure. It was explained in detail in the work of Casas et al.[5] that the description is especially challenging when the simulation considers only one column, which undergoes all steps sequentially as in our simulation code. Then the pressure p_{peq} has to be adjusted iteratively in such a way to guarantee the conservation of mass. The details of this procedure are not repeated in this work but are found in the work of Casas et al.[5] However, the two-column PSA experiments provide a good possibility to compare the pressure p_{peq} attained in the experiments with the one calculated in the simulations. This is shown in Figure 7 with the line indicating just the average value between p_{high} and p_{low}, whereas the asterisks and the circles indicate the values in the experiments and in the simulations, respectively. It is rather clear that both the experimental and the simulation results differ from the average value which is obvious considering the fact that pressure equalization causes desorption and adsorption at the same time in the two columns and both are governed by nonlinear isotherms. Furthermore, the direction of this deviation is predicted correctly by the simulation, but the absolute value of the deviation is too high in the simulation as compared to the experiments. This might be caused by the simplified description of the pressure equalization step. For instance, the piping between the two columns is not considered in the simulations; the ideal gas law is used and only the conservation of total mass and not that of the individual components is enforced. Moreover, in the simulations the pressure at the column inlet or outlet is kept constant and equal to the final pressure p_{peq} during the complete pressure equalization step which is a simplification compared to the experimental situation. Apart from these points, it is observed that the pressure p_{peq} in the simulation is quite sensitive to the value of the heat transfer coefficient h_L. As discussed above the latter is calculated according to a correlation used to describe all steps in the complete PSA cycle equally well. Therefore, it might be not optimal for the pressure equalization step. Furthermore, the resolution of the experimentally measured points is rather low compared to the short duration of the pressure equalization step (t_{peq} = 3 s) which makes an exact comparison between measured and simulated temperature profiles difficult. Because of these aspects and because of the fact that large scale PSA processes run close to adiabatic conditions, which will be adopted also in a simulation aiming at the optimization of such a process and reduces the influence of the parameter h_L, we believe that the procedure selected in our simulations for the description of the pressure equalization step is sufficiently correct.

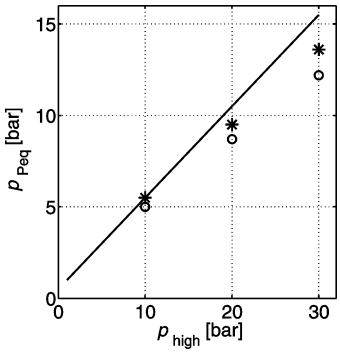

Figure 7. Pressure levels at the end of the pressure equalization step: (line) average value; (asterisk) experiments; (circles) simulation.

Description of the Piping. As already mentioned in the modeling part, in order to compare concentration profiles from experiments and simulations, the piping from the column outlet to the MS has to be carefully considered. In a first step, the piping is described by an isothermal plug flow model:

$$\frac{\partial c_i^{\text{pipe}}}{\partial t} + \frac{\partial (u^{\text{pipe}} c_i^{\text{pipe}})}{\partial x} - \frac{\partial}{\partial x}\left(D_{\text{pipe}} c_{\text{pipe}} \frac{\partial y_i^{\text{pipe}}}{\partial x}\right) = 0$$

$$i = 1, \ldots, I \tag{3}$$

$$\frac{\partial c_i^{\text{pipe}}}{\partial t} + \frac{\partial (u^{\text{pipe}} c_i^{\text{pipe}})}{\partial x} = 0 \tag{4}$$

The parameters used in this calculation are summarized in Table 4. The pipe length is taken directly from the experimental setup, whereas the pipe diameter is increased slightly with respect to the geometrical one in order to account for different parts of the piping system with a larger diameter such as flowmeters or valves. The dispersion coefficient is empirically selected in order to account for all effects in a lumped way. Consistent with the breakthrough study,[3] axial pressure drop is assumed to be negligible in the piping system. Furthermore, the pressure before the BPR (part 1 with length L_1) is assumed to be equal to the column outlet pressure at all times and the pressure after the BPR (part 2 with length L_2) equals the ambient pressure. In order to ensure the conservation of mass, the velocity at the BPR is recalculated accordingly. As initial conditions in the pipe for every new blowdown or adsorption step, we use the conditions at the end of the previous CO_2 or H_2 production step, respectively. This is true except for the first part of the piping used in the blowdown step. In this case, the composition in the pipe is altered by the preceding pressure equalization step, and therefore to account for this, the initial composition is adapted accordingly over a length of the piping corresponding to $L_1/2$ (see Table 4).

Table 4. Parameters to Describe the Piping

length before BPR	L_1	[m]	1.5
length after BPR	L_2	[m]	4.0
pipe diameter	d_{pipe}	[m]	0.008
pipe temperature	T_{pipe}	[K]	298
pipe dispersion coefficient	D_{pipe}	[m^2/s]	0.001

Concentration Profiles of the CO_2 and H_2 Product. In Figure 8 the experimental results for the CO_2 and H_2 product (symbols) during one cycle at 20 bar are compared to the simulation results directly after the column (light gray solid line) and the results obtained after the piping (dark gray dashed−dotted line). Looking first at the CO_2 product in Figure 8a, it is obvious that there is a large discrepancy between experiment and simulation. Moreover, the influence of the piping is rather small, especially during the blowdown step. This is caused by the fact that the velocity at the beginning of the blowdown is quite high resulting in a very short time required for the gas to travel through the piping.

In order to analyze this discrepancy further, in a second step additionally to the simple piping, a stagnant "tank", which is in constant exchange with the column outflow, but not completely purged, is included in the model. This tank is characterized by a volume V_{Tank} and by the exchange rate with the flow out of the column into the piping. This concept seems reasonable, because between the column outlet and the BPR a kind of piping network exists, which is for instance used in the pressure equalization step as illustrated in Figure 1. Moreover, the pressure sensor installed at the column outlet adds further stagnant dead volume. In a previous study,[12] it has already been shown that such effects play an important role in the description of breakthrough experiments performed in a smaller column. The aim of this study is to evaluate the effect of such a "tank" and to see if it can explain the discrepancy between the simulations and the experiments. For the implementation the following assumptions are additionally taken. First, the pressure and temperature in the tank are assumed to be equal to the pressure and temperature (isothermal) in the first part of the piping. Second, the initial composition in the tank at the beginning of every blowdown step is equal to the composition at the end of the pressure equalization step. During the blowdown and purge step, this composition is changing continuously due to the exchange with the inlet flow of the piping.

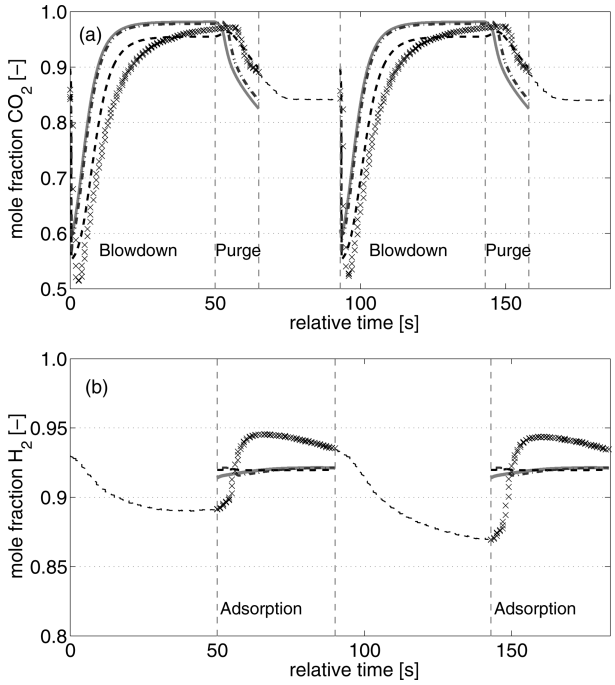

Figure 8. Comparison of CO_2 (a) and H_2 (b) profiles at 20 bar: simulation and experiment at steady state: (solid line) simulation directly after the column; (dashed−dotted line) simulation after the piping; (dashed line) simulation after the piping including a stagnant tank at the beginning of the piping; (symbols) experiments.

Using this modeling approach, indeed the experimental concentration profiles can be reproduced better as shown by the black dashed line in Figure 8a. However, this result is only obtained using a rather big tank volume and a very high exchange rate, i.e. an exchange rate of 98% and a tank volume of $V_{\text{Tank}} = 2 \times 10^{-5}$ m^3. This evaluation shows clearly that the comparison of simulated concentration profiles with experimental results measured after the piping is not trivial. Different aspects play a role, and it is not easy to describe all of them rigorously. Therefore, such results have to be evaluated with caution.

The same evaluation for the H_2 product is illustrated in Figure 8b. In this case the difference between the simulation just after the column, the one including the piping only and the results adding the stagnant "tank" is less pronounced. This results from the fact that the concentration at the column outlet in the simulation is rather constant during the complete adsorption step. Comparing these simulation results with the experimental data two further aspects have to be discussed. First, as explained already in the discussion of the experimental

results, the initial part of the H_2 product (steep increase) is affected a lot by the measurement procedure and the setup. As these effects are not included in the model, experiments and simulations cannot be compared properly. Second, it is clear that in the experiments a higher H_2 concentration is observed than in the simulations. This looks surprising, but on the other hand measuring highly concentrated H_2 with the MS is challenging. In fact, in independent measurements using H_2/CO_2 mixtures with known composition and applying the same calibration procedure as in the PSA experiments, it is observed that for mixtures with a similar high H_2 content, i.e. 95%, the measured result is 1−2% higher; such deviation would already be sufficient to explain the discrepancy between simulations and experiments.

From this analysis it follows that also in the case of the H_2 product the comparison between simulations and experiments is not straightforward. However, as we argued earlier, we believe that a reliable validation of the simulations can be done by comparing its results in terms of temperature profiles inside the column with the experimental temperature measurements.

Process Performance. The results from the measurement of the H_2 product flow rate, and from the ensuing calculation of the product purities and capture rates, are summarized in Table 2 along with the step times. They are also shown in Figure 9, together with the predictions based on simulations. For short times of the adsorption step, a high purity of the H_2 product is measured, along with a high CO_2 recovery; the H_2 recovery and CO_2 purity on the other hand are relatively low. This is due to the CO_2 front not advancing very far into the column during the adsorption step, leaving a portion of the column filled with H_2, which is withdraw along with the CO_2 during the blowdown and purge steps. Longer adsorption step times lead to a higher degree of saturation of the column, increasing the purity of the captured CO_2. After about 50 s, however, the CO_2 front reaches the end of the column, leading to a drop in its recovery. For t_{ads} = 100 s, the H_2 product contains a large amount of CO_2, and accordingly the CO_2 recovery is low. The change in product composition and flow rate posed a challenge for the measurement of the product flow rate for this experiment; therefore, it was repeated to verify the reproducibility. Along with the calculated values, error bars are shown which reflect the uncertainty of the measurement methods, namely the precision of the rotameter, for which a value of 1 mm is used, and the MS signal, as discussed in the previous section. These uncertainties are most evident in the measured CO_2 purity, as it is calculated indirectly. Figure 9 shows that the simulations correctly predict the trends seen for product purity and recovery. As seen in the experiments, adsorption step times of 60 s and longer result in CO_2 entering the H_2 stream leading to a higher purity of CO_2 at the cost of the capture rate. In particular the purity of the produced H_2 and the recovery of CO_2 are predicted rather well by the simulations.

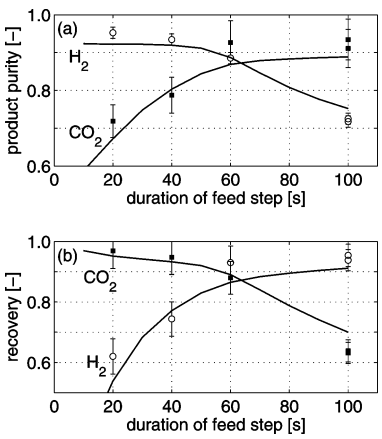

Figure 9. Simulated (−) and experimental (symbols) impact of the variation of the adsorption step time on the purity of the products (a) and on the recovery of both components (b) The error bars shown indicate the uncertainty in the measurement due to the limit of the precision of the rotameter used, as well as the uncertainty of the MS.

■ CONCLUSIONS

In this work PSA experiments aimed at separating H_2 and CO_2 using activated carbon are carried out in an automated laboratory two-column setup at 25 °C and at three different adsorption pressures, namely 10, 20, and 30 bar. The aim of this study is to provide a comprehensive experimental database in order to validate a process model, which can be used for the development of a PSA process in the context of precombustion CO_2 capture. This one-dimensional, nonisothermal, and nonequilibrium PSA model has been developed recently to describe single-column breakthrough experiments.[3] However, such breakthrough experiments only resemble very closely the conditions encountered in the adsorption step. The PSA experiments in this study are taken in order to assess the accuracy of the model concerning the other steps, particularly those exhibiting a change in pressure, namely pressurization, blowdown, and pressure equalization.

All experiments performed in this study exhibit an excellent level of reproducibility between different cycles, but also between the two columns as well as between experiments repeated under the same conditions. This is confirmed by comparing the temperatures measured inline at five specified positions and the concentration of the gas leaving the columns, which is measured online by mass spectrometry.

The comparison between simulations and experimental results is done by comparing on the one hand the concentration profiles of the gas leaving the columns. Due to the fact that the measured concentration profiles are influenced by the piping system between the column outlet and the MS and because a simple time correction of the experimental data is not possible, the piping is included in the model. The assessment of different model approaches shows that it is not trivial to account for this effect in a rigorous way. Consequently, it is not straightforward to compare measured concentration profiles with simulation results. Such data have to be treated with care.

On the other hand, the temperatures are measured without delay directly inside the columns at specified positions. Since the adsorption front comes along with a strong temperature increase caused by the heat of adsorption, it could be demonstrated that these temperature profiles provide a good basis for comparison of simulation and experimental results. Using the mass transfer coefficients fitted to the breakthrough experiments[3] and a heat transfer coefficient calculated according to Leva's correlation,[10,11] the experimental temperature profiles could be well described by the PSA model in the entire range of conditions that are evaluated.

The outcome of the research that we have presented in this work leads to some final considerations. The first regards the accuracy of the model in describing reality. Our conclusion is that once the model parameters are estimated in such a way

that the temperature profiles are accurately described, then also the compositions of the product streams are accurately predicted. This holds true despite the observed discrepancy in the concentration profiles between simulations and measurements that we attribute, as explained above, to experimental difficulties, which might be experienced in a similar way in any laboratory or pilot setup for pressure swing adsorption. The experimental determination of the process performance has shown that the trends in product purity and recovery are accurately predicted by the presented model, despite the discrepancy in the concentration profiles. The experimental challenges that were encountered during the measurement of the concentration also impacted these experiments, in that the piping downstream of the column causes a pressure drop that has an effect on the measurement of the flow rate. Despite that, the quantities of interest for process design could be determined, and the repetition of an experiment has shown that the results are reproducible.

Moreover, the study presented in this work provides a detailed analysis about the issues encountered when comparing simulations to experimental results. Though this is done for our specific setup, we think that the analysis bears general validity. In order to compare simulated concentration profiles with measurements, one has additionally to model the piping system and to account for different issues related to the up- or downstream equipment of a specific setup; in our case these are the difficulties in measuring high purity H_2 streams and in calibrating the mass flow meter and controller. In order to describe thermal effects in the adsorption column properly and accurately, when starting from a model with parameters fitted to breakthrough experiments, one has to fine-tune the values of the heat transfer coefficient and of the heat of adsorption. This is needed in order to better reflect the overall conditions during the whole PSA cycle, which are of course different from what prevails during single-column breakthrough experiments. It is shown that the way we do such fine-tuning is based on solid physical arguments.

■ ASSOCIATED CONTENT

Supporting Information

Equations of the model used, along with tables containing the parameters used in the model. Additionally, simulated internal profiles and detailed information about the experimental evaluation of process performance. This material is available free of charge via the Internet at http://pubs.acs.org/.

■ AUTHOR INFORMATION

Corresponding Author

*E-mail: marco.mazzotti@ipe.mavt.ethz.ch. Phone: +41-44-6322456. Fax: +41-44-6321141.

Notes

The authors declare no competing financial interest.

■ ACKNOWLEDGMENTS

The research leading to these results has received funding from the European Union's Seventh Framework Program (FP7/2007-2011) under grant agreement no. 211971 (the DECARBit project).

■ NOTATION

a = parameter for temperature dependent description of n_i^∞ [mol/kg]
A = parameter for temperature dependent description of k_i [1/Pa]
b = parameter for temperature dependent description of n_i^∞ [J/mol]
B = parameter for temperature dependent description of k_i [J/mol]
c = fluid phase concentration [mol/m^3]
C_{ads} = heat capacity adsorbed phase [J/(K kg)]
C_g = heat capacity gas mixture [J/(K m^3)]
$C_{g,i}$ = heat capacity gas [J/(K mol)]
C_s = heat capacity adsorbent [J/(K kg)]
C_w = heat capacity wall (lumped) [J/(K m^3)]
D = dispersion coefficient [m^2/s]
d = diameter [m]
d_p = particle diameter [m]
ΔH = heat of adsorption [J/mol]
h_L = heat transfer coefficient (lumping column inside + wall) [J/(K s m^2)]
h_w = heat transfer coefficient (wall to ambient) [J/(K s m^2)]
I = number of species [−]
k = isotherm equilibrium constant [1/Pa]
K_L = thermal conductivity in the fluid [W/(m K)]
L = column length [m]
L_1 = length of piping before BPR [m]
L_2 = length of piping after BPR [m]
n = molar adsorption per unit mass of adsorbent [mol/kg]
p = pressure [Pa]
R = ideal gas constant [J/(mol K)]
R_i = internal column radius [m]
R_0 = external column radius [m]
s = exponent in Sips isotherm [−]
t = time [s]
T = temperature [K]
u = superficial gas velocity [m/s]
V = volume [m^3]
x = space coordinate in axial direction [m]
y = mole fraction [−]

Greek Letters

α = parameter for temperature dependent description of exponents [−]
β = parameter for temperature dependent description of exponents [−]
ε_b = bed void fraction [−]
ε_t = total void fraction [−]
η_1 = parameter Nusselt correlation [−]
η_2 = parameter Nusselt correlation [−]
k = overall mass transfer coefficient [1/s]
μ = dynamic viscosity [Pa s]
ξ = factor in the function that describes the pressure decrease during blowdown [1/s]
ρ_m = fluid phase density (mass) [kg/m^3]
ρ_b = bed density [kg/m^3]
ρ_M = material density [kg/m^3]
ρ_p = particle density [kg/m^3]

Sub- and Superscripts

ads = adsorption step
amb = ambient
blow = blowdown step
high = high adsorption pressure
i = component i
j = component j
low = low pressure during purge

peq = pressure equalization step
Pipe = pipe
press = pressurization step
purge = purge step
ref = reference state for temperature dependent description of exponents
Tank = tank
w = wall
∞ = saturation (isotherm equation)
* = equilibrium

Abbreviations

BPR = back pressure regulator
CCS = carbon capture and storage
IGCC = integrated gasification combined cycle
MFC = mass flow controller
MS = mass spectrometer
Peq = pressure equalization
PSA = pressure swing adsorption
WGS = water gas shift

■ REFERENCES

(1) IPCC. *IPCC Special Report on Carbon Capture and Storage*; Cambridge University Press: Cambridge, U.K., 2005.
(2) Farooq, S.; Ruthven, D. M. Heat Effects in Adsorption Column Dynamics. 1. Comparison of One- and Two-Dimensional Models. *Ind. Eng. Chem. Res.* **1990**, *29*, 1076.
(3) Casas, N.; Schell, J.; Pini, R.; Mazzotti, M. Fixed bed adsorption of CO_2/H_2 mixtures on activated carbon: experiments and modeling. *Adsorption* **2012**, *18*, 143.
(4) Schell, J.; Casas, N.; Pini, R.; Mazzotti, M. Pure and binary adsorption of CO_2, H_2, and N_2 on activated carbon. *Adsorption* **2012**, *18*, 49.
(5) Casas, N.; Schell, J.; Joss, L.; Mazzotti, M. A parametric study of a PSA process for pre-combustion CO_2 capture. *Sep. Purif. Technol.* **2013**, *104*, 183.
(6) Yang, R. *Gas separation by adsorption processes*; Imperial College Press: London, 1987.
(7) Park, J.-H.; Kim, J.-N.; Cho, S.-H. Performance analysis of four-bed H_2 PSA process using layered beds. *AIChE J.* **2000**, *46*, 790.
(8) Yang, R.; Doong, S. Gas Separation by Pressure Swing Adsorption: A Pore-Diffusion Model for Bulk Separation. *AIChE J.* **1985**, *31*, 1829.
(9) Cen, P.; Yang, R. T. Separation of a Five-Component Gas Mixture by Pressure Swing Adsorption. *Sep. Purif. Technol.* **1985**, *20*, 725.
(10) Leva, M. Heat Transfer to Gases through Packed Tubes. *Ind. Eng. Chem.* **1947**, *39*, 857.
(11) Ruthven, D. *Principles of Adsorption and Adsorption Processes*; John Wiley & Sons, Inc.: New York, 1984.
(12) Joss, L.; Mazzotti, M. Modeling the extra-column volume in a small column setup for bulk gas adsorption. *Adsorption* **2012**, *18*, 381.
(13) NIST. *NIST Chemistry WebBook*, 2012; webbook.nist.gov/chemistry. (Accessed June 5, 2013).
(14) *NIST Reference Fluid Thermodynamic and Transport Properties Database (REFPROP)*, Version 9.0; National Institute of Standards and Technology: Gaithersburg, MD, 2011.